A Dual Six-Port Automatic Network Analyzer

HARRY M. CRONSON, SENIOR MEMBER, IEEE, AND LEON SUSMAN, SENIOR MEMBER, IEEE

***Abstract*—A 2- to 18-GHz dual six-port automatic network analyzer using diode power detectors is described. An analysis of the calibration technique is discussed in detail. Measurement accuracies of better than 0.1-dB up to 40-dB insertion loss from 2 to 7 GHz are reported. Possible causes of the errors observed at higher frequencies are given.**

I. Introduction

Almost ten years ago, Hoer and Engen at the National Bureau of Standards (NBS) began to investigate the six-port junction as the heart of a simpler and less expensive network analyzer [1], [2]. Since then there has been considerable work in the analysis, design, and testing of six-port systems. This evolution has included both single six-port reflectometers for one-port measurements and dual six-ports for two-port measurements.

The use of a dual six-port system was first proposed by Hoer in 1977 [3]. In keeping with the philosophy of the six-port measurement art, calibration and measurement procedures which require a minimum of known standards were sought. At least three such approaches have been developed and refined over the past three years. The first of these was described by Hoer [4]. Its major disadvantage was the restriction to components with sexless connectors. This limitation was removed by a procedure proposed by Susman [5] who showed that a Through, Short, and Delay connection (TSD) at the terminals of the two six-ports were sufficient to calibrate each six-port. At about the same time, Engen showed that the six-port network could be mathematically reduced to an equivalent four-port [6]. His incorporation of the TSD error correction technique, developed by Franzen and Speciale [7], resulted in a completely different mathematical procedure for calibrating the dual six-port [8]. Most recently, Engen and Hoer have modified this technique by removing the requirement for a known short circuit in favor of an unknown reflecting sexless one-port [9]. They called this procedure TRL for through-reflect-line. A recent dual six-port system with thermistor power detectors showed exceptional performance at 3 GHz [10] using the TRL calibration.

In this paper, we describe a diode based dual six-port analyzer built for the U.S. Army Metrology and Calibration Center (AMCC). The modified TSD calibration procedure used for this system is reviewed in detail in Section II. Section III contains a description of the system while the experimental results obtained to date are presented in Section IV. Our experience with this system has shown that there is considerable art required in the construction and proper utilization of the dual six-port system, and some subtle questions need to be answered before six-port technology can be confidently taken from the research laboratory.

Manuscript received May 16, 1980; revised December 1, 1980. This work was supported by the U S Army Missile Command, Redstone Arsenal, AL under Contract DAAH01-77C-0693 A condensed version of this paper has been presented at the 1980 IEEE-MTT-S International Symposium, Washington, DC.

The authors are with Sperry Research Center, Sudbury, MA 01776

II. Analysis

A. Matrix Description

The TSD calibration procedure can be described by matrix equations. The resulting compact notation is helpful in gaining insight among the fundamental relations.

Consider the network configuration shown in Fig. 1 consisting of two six-port networks excited by a signal from a common source. Each six-port has four power detectors attached to their respective outputs. The variable attenuator and phase shifter are used to vary the complex ratio of incident signals on the two networks. For each six-port network we can write a linear matrix relationship between the power readings and certain quadratic functions associated with the scattering variables of the six-port. In particular, the following matrix equations are valid for the two networks:

$$\boldsymbol{a}_{q1} = C_1 \boldsymbol{p}_1 \qquad \boldsymbol{a}_{q2} = C_2 \boldsymbol{p}_2 \tag{1a}$$

where the column matrices $\boldsymbol{a}_{q1}$ and $\boldsymbol{a}_{q2}$ are defined by

$$\boldsymbol{a}_{q1} \equiv \begin{bmatrix} |a_1|^2 \\ a_1 b_1^* \\ a_1^* b_1 \\ |b_1|^2 \end{bmatrix} \qquad \boldsymbol{a}_{q2} \equiv \begin{bmatrix} |a_2|^2 \\ a_2 b_2^* \\ a_2^* b_2 \\ |b_2|^2 \end{bmatrix}. \tag{2}$$

The column matrices $\boldsymbol{p}_1$, $\boldsymbol{p}_2$ contain 4 power readings from networks 1 and 2, respectively. Matrices C_1, C_2 are 4×4 complex matrices whose entries are the calibration constants for networks 1 and 2, respectively. Equation (1a) is the basic relation between the observable power readings and the input quantities defined by (2). The entries of $\boldsymbol{a}_{q1}$ and $\boldsymbol{a}_{q2}$ are quadratic functions of the scattering variables a_1, b_1 and a_2, b_2 associated with reference planes at each six-port.

0018-9480/81/0400-0372$00.75 © 1981 IEEE

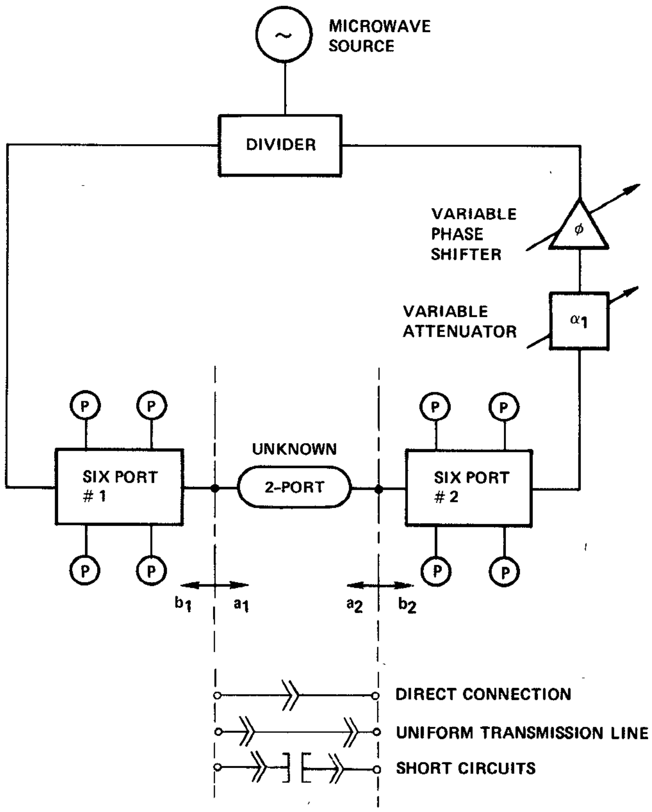

Fig. 1. Dual six-port configuration.

By placing a two-port network between the two six-ports we can constrain the matrices $\boldsymbol{a}_{q1}$ and $\boldsymbol{a}_{q2}$ to satisfy an equation of the form

$$\boldsymbol{a}_{q1}=T_q\boldsymbol{a}_{q2} \tag{3a}$$

where the entries of T_q are related to the transfer matrix of the two-port. The calibration constants of the dual six-port are obtained using a through-short-delay procedure described in [5]. It is reviewed here to clarify the underlying assumptions and to expand its range of applicability.

B. Calibration Procedure

The calibration procedure consists of three steps wherein certain "standards" are inserted between the two six-port networks and the resulting power readings are acquired. These readings are used to solve equations whose solution are the calibration constants. In the first step the two six-port networks are connected directly together as symbolically shown in the lower part of Fig. 1. This results in eight power readings, which are stored in the column matrices $\boldsymbol{p}_1$ and $\boldsymbol{p}_2$. This procedure is repeated for a different external state obtained by changing the variable phase shifter and/or attenuator settings. These settings need not be known exactly but must be chosen so that the column matrices $\boldsymbol{a}_{q1}$ and $\boldsymbol{a}_{q2}$ are linearly independent. In theory only four external states are needed, but to obtain the benefits of redundancy six external states are used. Thus a total of 48 power readings are taken. The results of these measurements can be described by an expansion of equation (1a)

$$A_1=C_1P_1 \qquad A_2=C_2P_2 \tag{1b}$$

where A_1 and A_2 are 4×6 matrices whose unknown columns are defined by equation (2) and P_1, P_2 are 4×6 matrices whose columns contain the corresponding power readings.

The relation between A_1 and A_2 follows from equation (3a)

$$A_1=T_qA_2. \tag{3b}$$

For this direct connection T_q takes the simple skew diagonal form

$$T_q=\begin{bmatrix}0&0&0&1\\0&0&1&0\\0&1&0&0\\1&0&0&0\end{bmatrix}. \tag{4a}$$

The calibration continues by replacing the direct connection with a length of uniform transmission line. The measurement sequence of 48 power readings is repeated which lead to new equations with different power matrices P_1', P_2' and a new matrix, T_q'. These are

$$A_1'=C_1P_1' \qquad A_2'=C_2P_2' \tag{1c}$$

$$A_1'=T_q'A_2' \tag{3c}$$

$$T_q'=\begin{bmatrix}0&0&0&e^{-2\alpha l}\\0&0&e^{+2j\beta l}&0\\0&e^{-2j\beta l}&0&0\\e^{+2\alpha l}&0&0&0\end{bmatrix} \tag{4b}$$

where the transmission line is assumed to have length l and propagation constant $\gamma=-\alpha+j\beta$. The transmission line may be coaxial or waveguide but in general should be a single mode structure so that its characteristic impedance is well defined. The length and propagation constant of the transmission line need not be known. However, the length l should not be a multiple of a quarter wavelength at the operating frequency.

The above equations can be solved for either calibration matrix C_1 or C_2. Specifically by eliminating C_2 the following similarity transformation is derived:

$$C_1\left[(P_1'P_2'^T)(P_2'P_2'^T)^{-1}(P_2P_2^T)(P_1P_2^T)^{-1}\right]C_1^{-1}=T_q'T_q \tag{5a}$$

or

$$C_1[A]C_1^{-1}=T_q'T_q \tag{5b}$$

where C^{-1} denotes the inverse of C and the product $T_q'T_q$ is a diagonal matrix. It is well known in matrix analysis [11] that (5b) is an eigenvalue equation. The calibration constants (the rows of C_1) are the eigenvectors of $[A]$ which are derived from known power readings. The eigenvalues are the diagonal entries of T_qT_q'. Since eigenvectors are only determined up to a multiplicative constant, the matrix C_1 is thus far determined up to a multiplicative diagonal matrix.

One additional measurement is needed to determine the multiplicative constants. This can be seen from the following analysis. Note that the reflection coefficient at each six-port is b_1/a_1 and b_2/a_2. From equations (1a) and (2), one can write for six-port network 1 that

$$\Gamma_1 = \frac{b_1}{a_1} = \frac{a_1^* b_1}{|a_1|^2} = K_1 \frac{\sum_{j=1}^{4} c_{3j} p_j}{\sum_{j=1}^{4} c_{1j} p_j} \tag{6}$$

where c_{3j} and c_{1j} are the third row and first row entries of C_1. A similar expression can be written for Γ_2, the reflection coefficient of six-port network 2. The constants K_1 and K_2 can be obtained by measuring a known impedance standard. In this procedure a short circuit with $\Gamma = -1 + j0$ has been used. If the power readings resulting from a short circuit on each of the six-ports is denoted as $p_j^{(s)}$, then from (6) the unknown constant K_1 is simply

$$K_1 = -\frac{\sum_{j=1}^{4} c_{1j} p_j^{(s)}}{\sum_{j=1}^{4} c_{3j} p_j^{(s)}} \tag{7}$$

with a corresponding equation for K_2. The short circuit measurement, which requires eight power readings, not only determines the constants K_1 and K_2 but physically determines the electrical reference planes from which the S-parameters of an unknown two-port are measured.

C. Measurement Procedure

The measurement procedure consists of inserting an unknown device under test (DUT) between the two six-ports. Each six-port has been calibrated as a reflectometer and it is well understood that measurement of the eight power readings for three external states is sufficient to calculate the S-parameters of the DUT [3].

For measuring a one-port network only one external state is required. The resulting reflection coefficient follows directly from (6).

D. Numerical Analysis Considerations

The central task in determining the calibration constants is to compute the eigenvalues and eigenvectors of the matrix of power meter readings given in (5a). This is relatively straightforward, as long as the four eigenvalues, $e^{+2\alpha l}, e^{-2\alpha l}, e^{+2j\beta l}, e^{-2j\beta l}$, are distinct. Distinct eigenvalues result if l is not a multiple of a quarter wavelength and $\alpha \neq 0$. When these conditions are met there are numerous techniques for finding the corresponding eigenvectors. The Sperry software uses an algorithm due to Faddeeva [12] for determining the eigenvalues and eigenvectors. In practice, the eigenvalues are always distinct since they are calculated from actual power readings of finite resolution. However as the lossless case is approached, unstable estimates of the eigenvectors result. Computer simulations have verified that this difficulty is caused by the finite resolution of the power readings. Alternate numerical methods have been tried, but to date no reliable algorithm has been found which can operate on actual power readings when a lossless line is used. To circumvent these numerical difficulties a lossy airline is used to calibrate the dual six-port. This delay line introduces approximately 1 dB of loss which is sufficient to stabilize the numerical process. The VSWR of the line is less than 1.05 over the 2- to 18-GHz band. The assumption that the delay line be nonreflecting is thus reasonably well approximated. However, the lossy line has a complex characteristic impedance. The normalization level of the resulting S-parameter measurement is thus complex instead of the desired 50-Ω level. This led to an examination of the renormalization problem.

E. Renormalization Techniques

Equations (4a) and (4b) are a mathematical representation of two "standards" needed to calibrate the dual six-port. There is however a subtle implicit assumption in this model. The scattering matrix and the transfer matrix of a two-port network is defined with respect to normalizing numbers at each of its ports. It is usually assumed that these normalizing numbers are simply a real impedance R_0, which is typically 50 Ω. Under this condition (4b) is a valid representation of a uniform, lossless transmission line. However a lossy transmission line has a complex characteristic impedance and (4b) is no longer strictly valid. For the low-loss transmission line used here the discrepancy in S-parameter measurements is usually small and has been neglected in this system.

Renormalization of a scattering matrix has been investigated in depth by Woods [13], [14] who derives the required results through a voltage wave approach. Using his methods it appears possible to calibrate the six-port with a lossy line and then to renormalize to a 50-Ω level by reflection measurements on a 50-Ω matched load.

III. System Description

The Sperry Dual Six-Port Automatic Network Analyzer (DSPANA) was designed to operate over the 2- to 18-GHz frequency range. Fig. 2 is a photo of the complete system. From the top of the cabinet, the instruments are a frequency counter with phase lock capability, a scanner, digital voltmeter (DVM), RF sweeper, and a microwave drawer including one six-port junction. The other six-port is exterior to the cabinet, so that the DUT can be connected between the two six-ports. All instruments are controlled by the desk-top computer. Upon program command the RF sweeper is set to a specified frequency. The counter measures the actual frequency and phase locks the generator. The scanner controls the seven mechanical switches and multiplexes the eight diode outputs into the DVM.

The dual six-port microwave configuration is shown in Fig. 3. This network consists of two six-port junctions along with other components for calibration and measurement. All the lines shown are 0.141 in outside diameter

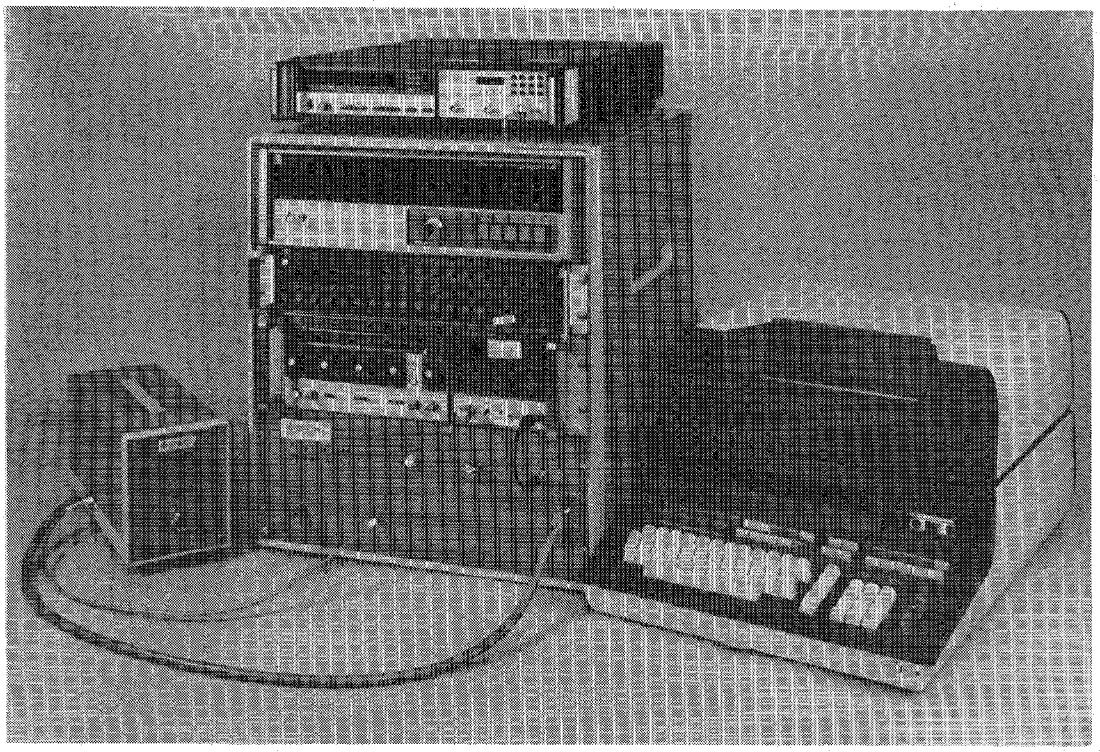

Fig. 2. The Sperry dual six-port automatic network analyzer.

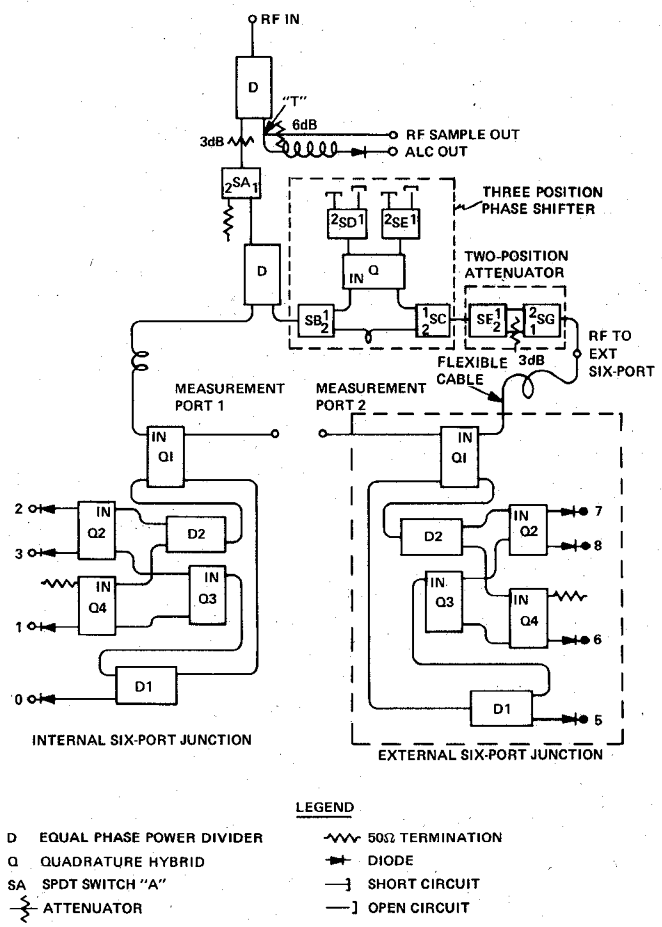

Fig. 3. Dual six-port microwave configuration.

semirigid coaxial cable. Tracing this circuit from the top, the RF input is split by an equal phase power divider (D) into two paths. One path is used for monitoring going through an unmatched coaxial tee via a 6-dB attenuator to the RF SAMPLE OUT port where it is connected by a cable to the frequency counter. The other port of the tee is used for leveling and is connected through a delay line and diode to the ALC (automatic leveling control) OUT port. The delay line of approximately 15 ft was inserted on the RF side of the diode to compensate for line losses between this point and the measurement ports so that the power entering the DUT would be leveled to within a few decibels over the entire 2- to 18-GHz frequency range. Continuing with the other port of D, the signal goes through a 3-dB attenuator and into the first single pole double through switch designated as SA. This component is included to switch power away from the main circuits and into the 50-Ω termination on its output port 2. With the switch in this position, the offset voltages of the diodes in the system are acquired for subsequent subtraction from the diode voltages with power applied. In position 1 the signal passes into another D where it is now split to pass to the two six-port junctions.

The left path to MEASUREMENT PORT 1 is entirely internal to the microwave drawer and goes through a delay line about 7 ft in length. This line was inserted to reduce frequency sensitivity by line length equalization. The six-port junction is fabricated from four quadrature hybrids (Q) and two dividers. The coaxial lines in the junction are also equalized so that with a short at the measurement

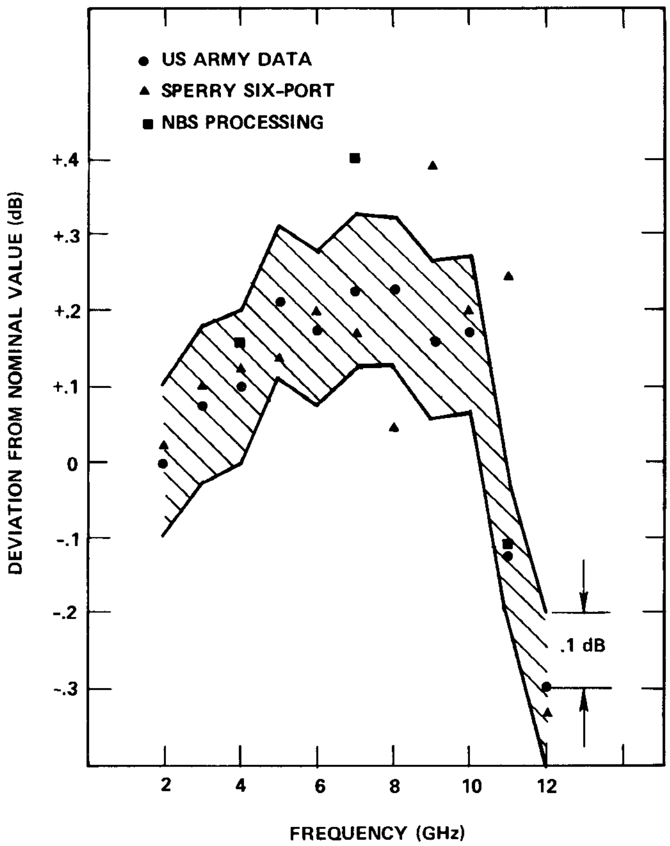

Fig. 4. $|S_{21}|$ measurement accuracy of 30-dB type N attenuator.

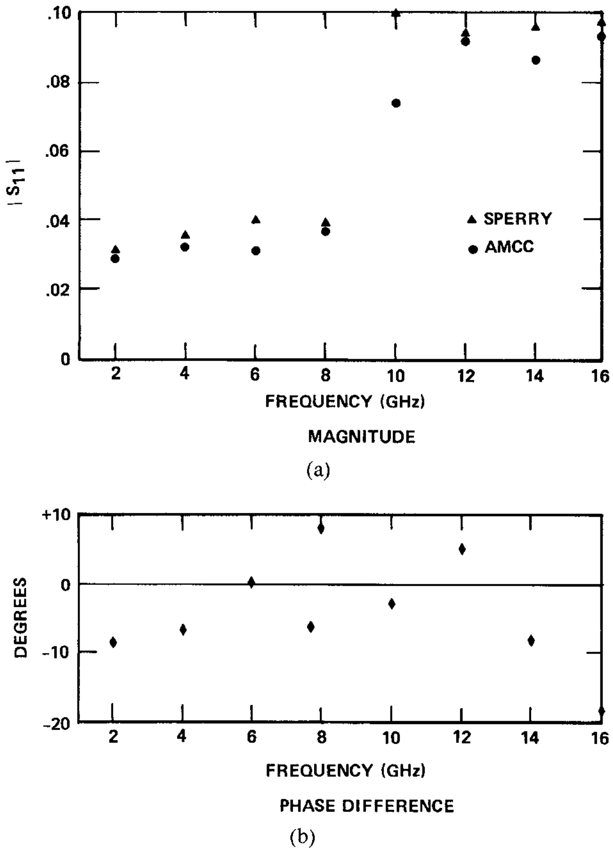

Fig. 5. $|S_{11}|$ measurement accuracy of 3-dB, APC-7 attenuator.

port, an impulse signal entering the IN port of $Q1$ and subsequently reflected from the short will arrive at ports 1, 2, and 3 at the same time. The diodes on these ports are mounted in a temperature controlled aluminum block. Returning to the right leg of the configuration, the signal passes through two networks inside the microwave drawer that produce six discrete states of amplitude and phase into MEASUREMENT PORT 2. The first network with four switches and a Q was designed to produce phases of 0°, +90°, and −90° over the 2- to 18-GHz range. The second network comprising two switches and an attenuator serves as a two step attenuator with 0- and 3-dB states. The output of the two step attenuator goes to the RF TO EXT SIX-PORT output on the front panel. The RF signal passes through a 3-ft flexible cable into the external six-port. The construction of the external six-port is similar to the internal one.

IV. System Performance

The system performance of the DSPANA was evaluated by calibrating the system and measuring various two-port passive components. The measurements indicated that accuracies of better than 0.1 dB could be obtained up to 40-dB insertion loss from 2 to 7 GHz. Above this frequency, results were more erratic. The dynamic range was about 50 dB. Some examples of the observed measurement accuracy are given below.

Fig. 4 illustrates three sets of data for $|S_{21}|$ of a 30-dB type N attenuator. The filled circles are calibration points taken by AMCC. These are assumed to be the correct values and a ±0.1-dB cross-hatched error band has been placed around them. The filled triangles are the data taken on the Sperry system. At 4, 7, and 11 GHz, we show filled squares for NBS processed data which came from calibration and measurement power readings taken on the Sperry system and processed at NBS using their algorithms. Note that although most of the points fall within the ±0.1-dB band, there are larger deviations in the Sperry data at 8, 9, and 11 GHz. This behavior was fairly typical of all $|S_{21}|$ results.

An example of S_{11} data is shown in Fig. 5 for a 3-dB APC-7 attenuator. The data symbols for the magnitude are the same as described above except that no NBS processed data was taken. Here the difference in $|S_{11}|$ is less than 0.01, except at 10 GHz. The phase differences are less than ±10° through 14 GHz and less than −20° at 16 GHz.

One of the novel features of the dual six-port system is that components with various connectors can be measured without introducing errors due to adapters because the system can be calibrated with adapters in place for almost any connector combination. For example, we measured a 6-dB attenuator with a male N connector on each port. Since the measurement ports of the basic SPANA are equipped with a male N and female N connector, a double female N adapter was connected to the male N measurement port and left in place for the remainder of the

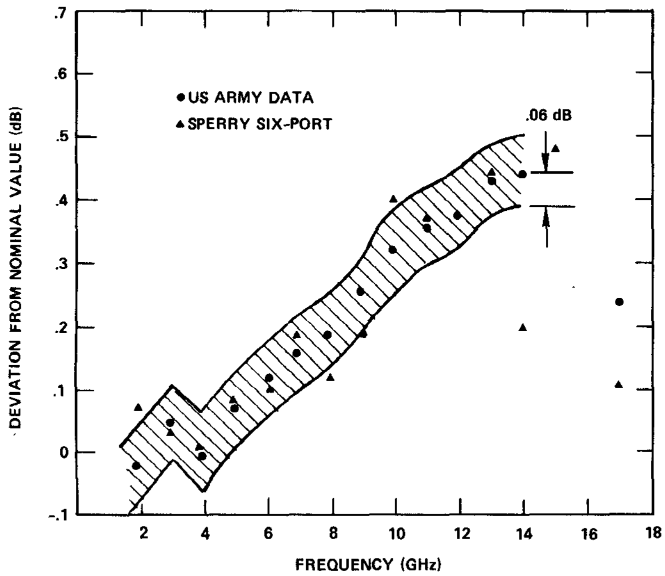

Fig. 6. $|S_{21}|$ measurement accuracy of 6 dB with double male N connectors attenuator.

TABLE I
20-dB ATTENUATOR REPEATABILITY

FREQUENCY (GHz)	2	3	4	5	6	7	8
AVERAGE (dB)	20.005	20.031	20.021	20.083	20.068	20.106	19.97
STANDARD DEVIATION (dB)	.033	.015	.0145	.0314	.0337	.631	.047
DEVIATION FROM CALIBRATED VALUE (dB)	-.035	-.006	-.011	+.042	+.032	.006	-.18

calibration and measurement procedure. The through measurement was made with a short section of lossless airline with a male N connector on each port. For calibrating with the lossy airline, the female N connector of the lossy line was replaced by a male N connector. After completing the calibration with shorts, we inserted the 6-dB attenuator with male N connectors on each port. Fig. 6 shows the results of insertion loss measurements with a ± 0.06-dB (± 1-percent) error band. Over the 2- to 13-GHz band, there is good agreement between the Sperry and AMCC values. Since the attenuator is only specified for use up to 12 GHz, the data suggests that the poor match above 12 GHz greatly influences the agreement.

To examine the long term behavior of the calibration constants, 10 measurements were made over a 14-day period. The 20-dB attenuator was measured almost daily using calibration constants stored on tape. Table I shows the repeatability with row 1 giving the average value over the 2- to 8-GHz band, row 2 listing the standard deviation, and row 3 showing the deviation from the calibrated values established by the U.S. Army for this component. Note that from 2 to 6 GHz both the standard deviation and deviation from calibrated values are quite small. At 7 GHz the standard deviation is large indicating perhaps a connect-disconnect problem. At 8 GHz the large deviation from the calibrated value may be due to errors in the stored calibration constants.

V. CONCLUSIONS

The main conclusion is that while the diode based system is capable of accurate measurements, some "bugs" remain. The most likely causes of the poorer agreement at higher frequencies are errors in the calibration procedure, the presence of harmonics in the signal source, and diodes not operating in the square law region. As discussed in Section II, the calibration procedure used requires a "reflectionless" lossy line for the solution of the eigenvalue calibration equation. In practice, the $\sim$1-dB lossy line does have a finite reflection coefficient of less than 0.025 from 2 to 18 GHz. Furthermore, it is known that since a lossy line has a complex characteristic impedance, it can never be perfectly matched to a real characteristic impedance. Thus, it is recommended that in a microwave coaxial system where nearly lossless delay standards are available, a calibration procedure that does not require a lossy line should be used. A test of the system with a calibration procedure using a lossless delay standard [9], would help in evaluating the error caused by the lossy line. It is interesting to note that in some proposed 94-GHz systems, a lossy delay standard will be difficult to avoid because of waveguide loss and renormalization will have to be introduced.

Two basic assumptions of six-port theory are single frequency operation and power measurements with the output detectors. With harmonics in the source, the equations which contain multiplications by the complex conjugate of the traveling waves no longer adequately describe the situation. Similarly, if the diodes are not operating in the square law range, their outputs will not be proportional to power. Both these error sources require additional investigation.

ACKNOWLEDGMENT

The authors appreciate the support and encouragement of Fred Seeley and Malcolm Shelton of the Army Metrology and Calibration Center, Huntsville, AL, and the cooperation of Cletus Hoer of NBS, Boulder, CO. The assistance of R. Mara and R. Sceppa in system fabrication is also gratefully acknowledged.

REFERENCES

[1] C. A. Hoer, "The six-port coupler: A new approach to measuring voltage, current, power, impedance, and phase," *IEEE Trans. Instrum. Meas.*, vol. IM-21, pp. 466–470, Nov. 1972.
[2] G. F. Engen and C. A. Hoer, "Application of an arbitrary six-port junction to power-measurement problems," *IEEE Trans. Instrum. Meas.*, vol. IM-21, pp. 470–474, Nov. 1972.
[3] C. A. Hoer, "A network analyzer incorporating two six-port reflectometers," *IEEE Trans. Microwave Theory Tech.*, vol. MTT-25, pp. 1070–1074, Dec. 1977.
[4] C. A. Hoer, "Calibrating two six-port reflectometers with only one impedance standard," NBS Tech. Note 1004, June 1978.
[5] L. Susman, "A new technique for calibrating dual six-port networks with application to S parameter measurements," in *IEEE MTT-S Int. Microwave Symp. Dig.*, 1978, pp. 179–181.
[6] G. F. Engen, "Calibrating the six-port reflectometer," in *IEEE MTT-S Int. Microwave Symp. Dig.*, 1978, pp. 182–183.

[7] N. R. Franzen and R. A. Speciale, "A new procedure for system calibration and error removal in automated *S* parameter measurements," in *5th European Microwave Conf. Proc.*, 1975, pp. 69–73.
[8] G. F. Engen, C. A. Hoer, and R. A. Speciale, "The application of 'thru-short-delay' to the calibration of the dual six-port," in *IEEE MTT-S Int. Microwave Symp. Dig.*, 1978, pp. 184–185.
[9] G. F. Engen and C. A. Hoer, "'Thru-reflect-line': An improved technique for calibrating the dual six-port," *IEEE Trans. Microwave Theory Tech.*, vol. MTT-27, pp. 987–993, Dec. 1979.
[10] G. F. Engen and C. A. Hoer, "Performance of a dual six-port automatic network analyzer," *IEEE Trans. Microwave Theory Tech*, vol. MTT-27, pp. 993–998, Dec. 1979.
[11] F. R. Gantmacher, *The Theory of Matrices*, Vol. 1. New York: Chelsea, 1960, p. 152.
[12] V. N. Faddeeva, *Computational Methods in Linear Algebra.* New York: Dover, 1959, p. 177.
[13] D. Woods, "Multiport network analysis by matrix renormalization employing voltage wave *S*-parameters with complex normalization," *Proc. Inst. Elec. Eng.*, vol. 124, no. 3, p. 198, Mar. 1977.
[14] D. Woods, "Multiport network analysis by matrix renormalization extension to four ports," *Proc. Inst. Elec. Eng.*, vol. 124, no. 9, p. 749, Sept. 1977.

Mode and Energy Guidance Properties of a Slab of Inhomogeneous Medium with Transverse Variations of the Gain Only

LAURA RONCHI ABBOZZO AND RICCARDO PRATESI

***Abstract*—The mode and energy guidance properties of a planar slab of parabolic graded index medium are examined when there are transverse variations of the gain or of the losses only.**

Mode configurations and propagation constants are evaluated of the first four even modes. The results are presented and discussed. In particular it is found that a gain decreasing away from the symmetry plane does not favor the existence of guided modes, as happens when the graded index medium is not limited to a slab. Evidence is found that the presence of the boundaries affects the mode propagation even when the caustic surface is well inside the slab.

I. Introduction

THE PURPOSE of the analysis described in the present paper is to study the mode guidance and the energy guidance properties, at optical frequencies, of a planar slab of graded index medium where there are transverse variations of the gain or of the losses only.

The possibility of mode guidance of an infinitely extended graded index medium (not limited to a slab) based on the transverse variations of the imaginary part of its refractive index has been extensively discussed by Marcuse [1]. In particular, Marcuse has shown that losses increasing or gain decreasing away from the symmetry plane $x=0$ may allow mode guidance even in "inverted" media, namely in media where the real part of the refractive index $\mathrm{Re}\, n(x)$ is an increasing function of the distance $|x|$ from the symmetry plane. By the term guided mode a beam is intended whose amplitude decays exponentially when $|x| \to \infty$. In the opposite case, the mode is termed "leaky".

When the graded index medium is limited to a slab, the situation appears different, at least in the ranges of parameters we have considered. For example, a gain decreasing away from the symmetry plane turns out not to favor the existence of guided modes (Section II). On the contrary, guided modes are found when the gain increases outwards. Another example is that the field amplitude distribution inside the slab turns out to be practically independent of the value of the parameter describing the transverse variations of the gain of the medium (Section III). These results seem to indicate that the mechanism of mode guidance of a slab is substantially different from that operating in the infinitely extended medium, and consequently, that the conclusions valid for the infinite medium cannot be simply extended to the case of a slab.

It is often suggested that, if a mode of the infinitely extended medium (whose amplitude has a Gaussian distribution, as is well known [1]) is sufficiently small where the slab has its boundaries, the presence of the boundaries does not substantially affect the mode distribution itself. This may be true, of course, but the question arises how

Manuscript received July 21, 1980; revised December 1, 1980.

L. Ronchi Abbozzo is with the Institute of Research on Electromagnetic Waves (I.R.O.E.), CNR, 50127 Firenze, Italy.
R. Pratesi is with the Quantum Electronics Laboratory (L.E.Q.), CNR, 50127 Firenze, Italy.

0018-9480/81/0400-0378$00.75 ©1981 IEEE